# A Study on PHF-Tau Network Effected by Apolipoprotein E4

Yuan Li, PhD[1], Zhijun Yao, PhD[2], Yongqing Yang, PhD[1],
Feng Zhao, PhD[3], Yu Fu, PhD[4], Ying Zou, MD[5],
and Bin Hu, PhD[2] ⓘ; Alzheimer's Disease Neuroimaging Initiative

## Abstract

Apolipoprotein E 4 Allele (APOE 4) is an important factors in Mild cognitive impairment (MCI) and Alzheimer's disease(AD). It plays a primary role in abnormal modification of aggregated Tau protein-paired helical filaments Tau (PHF-Tau). In this study, 143 subjects with PHF-Tau PET were divided into 2 groups (APOE 4 carriers and noncarriers). The measurements of the PHF-Tau network properties and resilient were calculated for 2 group networks respectively. APOE 4 carriers group showed significant differences in all the network properties in the results. We also found significant differences of betweenness centrality in some brain regions for APOE 4 carriers. Moreover, the APOE 4 carriers showed less resilient to targeted or random node failure. Our results indicated that the effects of APOE 4 may lead to abnormalities of PHF-Tau protein network. These findings may be particularly helpful in uncovering the pathophysiology underlying the cognitive dysfunction in MCI patients.

## Keywords

APOE 4, mild cognitive impairment, tau PET brain network, network properties, network resilience

## Introduction

Alzheimer's disease (AD) is a common neurodegenerative disease in the elderly, characterized by cognitive decline and short-term memory loss.[1] Mild cognitive impairment (MCI) is known as the prodromal stage of AD, accompanied by measurable impairment of memory, but general cognitive functioning is retained. Because the progression from MCI to AD is crucial, more and more studies have concentrated on MCI.[2] Previous study discovered that the paired helical Tau (PHF-Tau) protein is a highly disease-related factor that may induce the development of MCI and AD. The PHF-Tau was an attractive target for AD/MCI diagnosis and treatment.[3] Arnold et al revealed that accumulations of PHF-Tau neuro tangles in brain have been found in cases of definite AD.[4] Apolipoprotein E 4 Allele(APOE 4) has been proved to be a strong genetic risk factor affecting Alzheimer disease, which causes different types of brain networks abnormalities and short-term memory impairments.[5] It was revealed that the organization of metabolic network in APOE ε4 carriers indicated a less optimal pattern, suggesting that APOE 4 genotype might be a risk factor for MCI.[6] Although PHF-Tau and APOE 4 are all the important disease-related factors in MCI/AD, joint studies on the 2 factors are limited.

Positron Emission Tomography (PET) is an advanced clinical imaging technology in nuclear medicine. The general method of PET is to inject a substance, such as glucose, protein, nucleic acid and fatty acid, short-lived radionuclides labeled (e.g. 18F, 11C, etc.) into human body to detect the metabolic activity of life through the accumulation of the substance in metabolism, so as to achieve the purpose of diagnosis. The modern developments of neuroimaging technologies have made it a promising field to search certain neuroimaging

[1] School of Management Science and Engineering, Shandong Technology and Business University, Yantai, People's Republic of China
[2] School of Information Science and Engineering, Lanzhou University, Lanzhou, People's Republic of China
[3] School of Computer Science and Technology, Shandong Technology and Business University, Yantai, People's Republic of China
[4] College of Information Science and Electronic Engineering, Zhengjiang University, Hangzhou, People's Republic of China
[5] Department of Information Engineering, Yantai Vocational College, Yantai, People's Republic of China

**Corresponding Author:**
Bin Hu, University Roan, Science Park, Jinan, Shandong 250358, China; Tianshui Road, Lanzhou, Gansu 73000, China.
Email address: bh@lzu.edu.cn

biomarkers related to APOE4.[7] In recent years, 18F-AV-1451, the first novel PHF-Tau tracer (previously known as T807), have been demonstrated to detect tangle pathology in *vivo*.[8] It provide a new method to measure Tau neuronal tangles in the brain by in *vivo* neuroimaging. Cho et al pointed out that the tracer AV-1451 could be used to effectively measure the content of PHF-Tau in AD and MCI using PET images.[9]

Graph theory is a powerful framework that allows the representation of the brain as a complex network with interacting elements. It could provide a mathematical and conceptual framework to construct brain networks for exploring the topological patterns.[10] Previous study reported that topological abnormalities of human brain connectome were found in MCI patients, including major reorganizaiton of community structures and loss of small-worldness.[11] Wee et al demonstrated that the smaller small-worldness coefficients were found in the MCI group using fMRI. This result represented that brain networks were more random in MCI patients, a common characteristic of most neurodegenerative disorders.[12] Khazaee et al has been proved that the functional, regional and whole brain connections of patients with MCI were abnormal.[13] The study of large sample size and parametric investigation obtained from PET imaging are essential for detecting MCI-related abnormalities in brain networks.[14] However, the characteristics of the PHF-tau brain network affected by APOE 4 have not been explored extensively.

In this study, we hypothesized that the PHF-Tau protein network affected by APOE 4 is characterized by abnormal topological properties. By establishing the PHF-Tau network for the 2 groups introduced above, we attempted to investigate the alterations in topological patterns using the network-based algorithm. In conclusion, we hope this study could promote the general understanding of brain pathophysiological mechanism.

## Materials and Methodologies

### Ethics Statement

All AV-1451 PET images and Tau in CSF values were downloaded from the website of the Alzheimer's Disease Neuroimaging Initiative (ADNI; http://www.loni.ucla.edu/ADNI/). The major goal of the ADNI study is to track the progression of AD by using biomarkers to assess the brain's structure and function over the course of various states. The ADNI's data are gathered from 50 sites in the United States and Canada. The ADNI was launched in 2003 by the National Institute on Aging, the National Institute of Biomedical Imaging and Bioengineering, the Food and Drug Administration, private pharmaceutical companies, and nonprofit organizaiton as a 5-year public–private partnership. The lead author of this initiative is Michael W. Weiner, MD, University of California, San Francisco (Email ADNI: adni@loni.usc.edu). The data collections were proofread by each participating site's Institutional Review Board. Diagnostic criteria are stipulated at http://www.adni-info.org/Scientists/ADNIGrant/ProtocolSummary.aspx.

**Table 1.** Demographic Data of all Participants.

|  | APOE 4 carrier | APOE 4 noncarrier | P value |
|---|---|---|---|
| N(total N = 143) | 68 | 75 | – |
| Age | 76.27 ± 6.95 | 75.27 ± 4.19 | 0.4621[a] |
| Genger(male: female) | 35 ± 33 | 38 ± 37 | 0.8525[b] |
| MMSE | 25.7 ± 2.3 | 27.9 ± 1.7 | <0.001[a] |
| CSF-Tau | 251.3 ± 104.9 | 254.6 ± 128.2 | 0.89[a] |

Data are represented as the mean (standard) deviations.
[a]P value was obtained using the tt-test.
[b]P value was obtained using chi-square test.

### Subjects

All the 143 subjects, including those with MCI and normal controls (NC), were divided into 2 groups: APOE 4 noncarriers and APOE 4 carriers. APOE information was obtained from the ADNI database. MCI patients had reported a subjective memory concern either autonomously or through an informant or clinician. However, no significant level of impairment was present in other cognitive domains; essentially, their activities of daily living were preserved and no signs of dementia existed. Table 1 lists the demographic data of all subjects. In this study, each subject had an MMSE (Mini-mental State Examination, MMSE) score to measure the degree of mental state and cognitive impairment.

According to the prior knowledge, human with APOE gene can be divided into 2 cases including heterozygous(E2/E3, E3/E4, E2/E4) and homozygous(E2/E2, E3/E3, E4/E4). In our studies, the APOE 4 carriers contained 42 subjects with E3/E4 and 26 subjects with E4/E4, while the APOE 4 noncarries contained 21 subjects with E2/E3 and 54 subjects with E3/E3.

### Data Acquisition and Preprocessing

PET images were coregistered, averaged, normalized (standardized image and voxel size), and smoothed to a uniform resolution (8 mm full-width at half-maximum). PET scans required dynamic 30-min, six-frame (5-min each) acquisition starting 30 min after the injection of 18F-labeled AV-1451. We normalized all images spatially to the PET Montreal Neurological Institute (MNI) brain space template; subsequently, we scaled and averaged the same images by using Statistical Parametric Mapping 12 (SPM12: https://www.fil.ion.ucl.ac.uk/spm/software/spm12/) running under MATLAB 2014a on the Centos 6.5 operating system. The images used here were acquired using Siemens, GE, and Philips PET scanners in a resting state. The spatial normalization included a 12-parameter affine transformation; this process was followed by nonlinear iterative spatial transformation by using SPM12.

### Establishment of the Tau network

In graph theory, a network is composed of nodes and edges that connect a vertices sequence. In our study, graph theory-based

approaches were used to establish the PHF-Tau network of the 2 groups. A standardized automated anatomical labeling (AAL) template (90 brain regions in total, 45 in each cerebral hemisphere) was used to extract the brain regions. Subsequently, linear regression was performed to remove the effects of sex, age, and whole brain PHF-Tau levels on patients' measurements in each AAL brain region.[15] Three steps were adopted to estimate the correlation matrices. Firstly, we used the linear regression model to remove the effects of age, gender and the average value of whole-brain PHF-Tau protien level for each subject. Secondly, a correlation matrix R with dimensions $90 \times 90$ was generated, where every individual entry Rij was computed by the Pearson's correlation coefficient between region i and j. Finally, the correlation matrices were obtained with diagonal elements equivalent to 1. The number of total probable correlations were $90 \times (90 -1)/2$ for each group. In the PHF-Tau networks, the nodes and edges corresponded to the AAL areas and the undirected connections of the each pair in AAL areas, respectively. The topology of each group-network would differ significantly from each other under the thresholding of the same correlations value. In order to resolve this issue, sparsity (S) was used to threshold the correlations matrices of the networks into binarized matrices P, where an entry Pij equals 1 if |Rij| exceeded sparsity and 0 otherwise. The binary matrices Pij with N nodes and K edges were applied to simplify the metabolic networks, and reduce the computing scale for graph theory analysis. Sparsity was defined as the number of existing edges, K, divided by the maximum possible number of edges in a graph. There is no single optimal threshold selection method at present. We selected a sparsity value that ensures that all regions were included in the network, while minimizing the number of false positive connections as usual. So that it can be used to threshold each group's PHF-Tau network.

## Small-Worldness and Network Properties Analysis

Small-worldness was a property of complex networks that supported in all respects both modular and distributed dynamic processing as a principle of brain topology. For the small-worldness properties, clustering coefficients(and shortest path length(of the brain networks are compared with those of random networks which have the same number of nodes, edges, and degree distribution as the real networks.[16] Achieved the following standard could be called the small-worldness property: gamma = $Cp/Cp_{rand} \gg 1$, lambda = $Lp/Lp_{rand} \approx 1$ and sigma = gamma/lambda >1, where $Cp_{rand}$ and $Lp_{rand}$ referred to the Cp and Lp of a corresponding random network, respectively. In this study, random networks were repeated 300 times. In addition, global efficiency (Eglob) and local efficiency (Eloc) were also calculated. For global efficiency represents the inverse of the harmonic mean of the shortest path length between each pair of nodes, while local efficiency reflectes the information exchange efficiency between subgraphs.[17] As a brain network parameter, the modularity separates into smaller communities, with dense links within itself and minor links between them.[18] The quantity of modularity (Q) could be

accurately obtained using the greedy agglomerative algorithm. The Q is a benchmark for quantifying community detection performance,[19] and a high Q value indicates a robust division of the network. All of the network properties (Cp, Lp, Eloc, Eglob and Q) are computed using the Brain connectivity Toolbox (BCT).[20]

## Nodal Centrality Analysis

The "betweenness centrality" (BC) was defined as a local characteristic for exploring the outstanding nodes in the PHF-Tau networks. A node has a high betweenness which might bridge different parts of the network.[20] BC is equal to the number of shortest paths from all vertices to all others that pass through that node. The hub nodes played a crucial role in facilitating information communication and processing among the human brain networks. BC is normally used to select candidate hubs in a network. All central nodes and modules were calculated using the Brain Connectivity Toolbox (BCT).[20] The betweenness value of each node was computed at a fixed sparsity 8% to ensure that the brain network were fully connected without fragmentation in each group.

## Network Resilience Analysis

Being a crucial parameter of a complex network, network resilience refers to network stability and plasticity when losing nodes.[21] In PHF-tau brain network, the network resilience could be evaluated by removing the nodes in targeted and random patterns at the fixed sparsity 8%.[22] For the "targeted pattern analysis," we first computed the betweenness value of each node in the networks for the 2 groups respectively. Then, the nodes were deleted in decreasing sequence of their betweenness value. For the "random pattern analysis," the basic design principle was to delete nodes in a random order. The global efficiency of the damaged network is calculated and compared with the initial value of the unchanged network. As suggested in,[20] global efficiency is chosen to measure resilience.

## Statistical Analysis

The nonparametric permutation test was used to test the significant differences in PHF-Tau network properties between APOE 4 carriers and noncarriers such as Cp, Lp, Eglob, Eloc and Q value. In each fixed sparsity, the 2 groups properties were computed, pooled, and divided randomly into 2 randomized groups-APOE 4 carriers and noncarriers. In the process of the test, we kept the number of sampled carriers equal to the number of the original group. In each fixed sparsity, keeping the number of sampled carriers equal to the number of the original group, the 2 groups' properties were computed, pooled, and divided randomly into 2 randomized groups: APOE 4 carriers and noncarriers. Calculating the properties of each randomized group in every 5000 case with same sparsity threshold, we computed the differences in randomized groups, repeating 5000 times. At last, the 5000 recorded
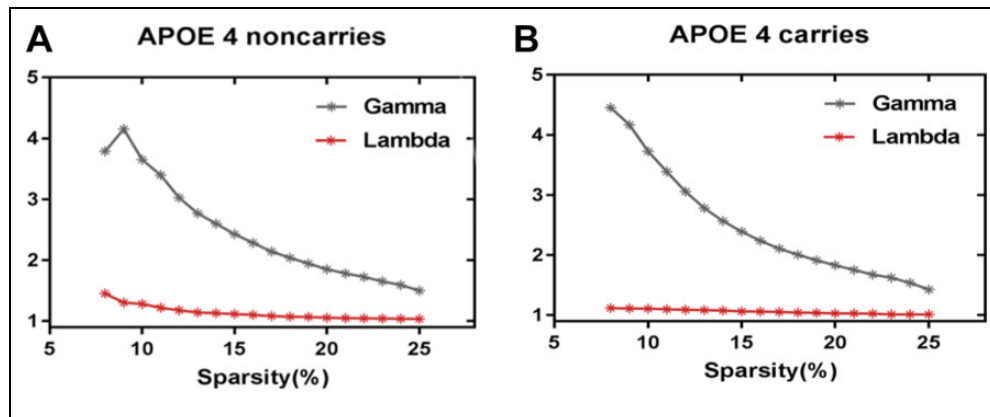
**Figure 1.** The small-worldness topology.

differences were sorted for finding the 2 groups differences in real PHF-Tau networks, which were included within 95% (2-tailed) in the supposed between-group differences.[23] If the real between-group difference was outside 95% confidence interval, we considered the 2 groups' networks had significant differences. In this study, we selected the sparsity threshold values ranging from $8\% < S < 25\%$(step = 1%) in this permutation test procedure. False discovery rate (FDR) was used to correct for these results.

## Results

### Demographic Characteristics

No significant differences were found in age or sex between the 2 groups. However, MMSE differed significantly between the 143 APOE 4 carriers and APOE noncarriers ($P < 0.05$). In addition, there was no significant difference in CSF-tau values between the 2 groups. In this research, we studied the effect of APOE 4 on PHF-Tau network without any difference in controlling other variables (Table 1). All the PET images for the APOE 4 carriers and noncarriers were shown in supplement materials.

### Small-Worldness and Network Properties

As showed in Figure 1, over the sparsity range of 8%-25% (step = 1%), both groups exhibit small-worldness topology (gamma>1, and lambda ≈1). Compared with APOE 4 noncarriers, the Cp and Lp of APOE 4 carriers are signifcantly decreased (sparsity = 9%-17%) (Figure 2A and 2B). Eloc of APOE 4 carriers is signifcantly increased (sparsity = 8%-10%) and Eglob of APOE 4 carriers is signifcantly increased (sparsity = 8%-16%) (Figure 2D and 2E), Q (sparsity = 9%, 15%-16%) (Figure 2C).We applied 5 thousand permutation tests to find the statistically significant differences between APOE 4 carriers and noncarriers in these properties. All of the above properties have significant differences in their low sparsities between APOE 4 carriers and noncarriers (Figure 2).

### Nodal Centrality Differences

In this study, we compared the differences between the 2 groups in nodal centrality. The results were shown in Table 2 and Figure 3. Compared with the APOE 4 noncarriers, the APOE 4 carriers showed increased regions which were in the right inferior frontal gyrus (triangular part), right superior frontal gyrus (dorsolateral), right middle frontal gyrus, right inferior occipital gyrus and right parahippocampal gyrus, whereas decreased regions were observed in right inferior temporal gyrus, left middle temporal gyrus, left superior parietal gyrus ($P < 0.05$; FDR). In the Table 2, X, Y, Z represented the three-dimensional coordinates of specific regions in the brain, and P values indicated the significance of the difference. The P values were all less than 0.05, reflecting significant differences in APOE 4 carriers.

### The Comparison of Network Resilience

As seen in Figure 4, the global efficiency was decreased as the deletion ratios growing in the 2 groups. In both networks, compared with APOE 4 noncarriers, APOE 4 carriers have a faster rate of decline in global efficiency over a wide percentage of removal. We also observed that the performances of the 2 groups were interwoven near the end of the removal processes in both patterns. Responding to the failures and crashes, the PHF-tau network resilience in APOE 4 noncarriers group are more stable than APOE 4 carriers group.

## Discussion

In this study, we explored different topological organizations of PHF-tau network in APOE 4 carriers and noncarriers groups. There were 3 main findings: (1) Compared with APOE 4 noncarriers, APOE 4 carriers displayed losses of small-worldness, changed global topological organization; (2) Regions with significant decreased nodal centrality were mainly distributed in frontal region, parietal region and temporal region in APOE 4 carriers; (3) The PHF-network of APOE 4 noncarriers group would be more stable than that of APOE 4 carriers group.
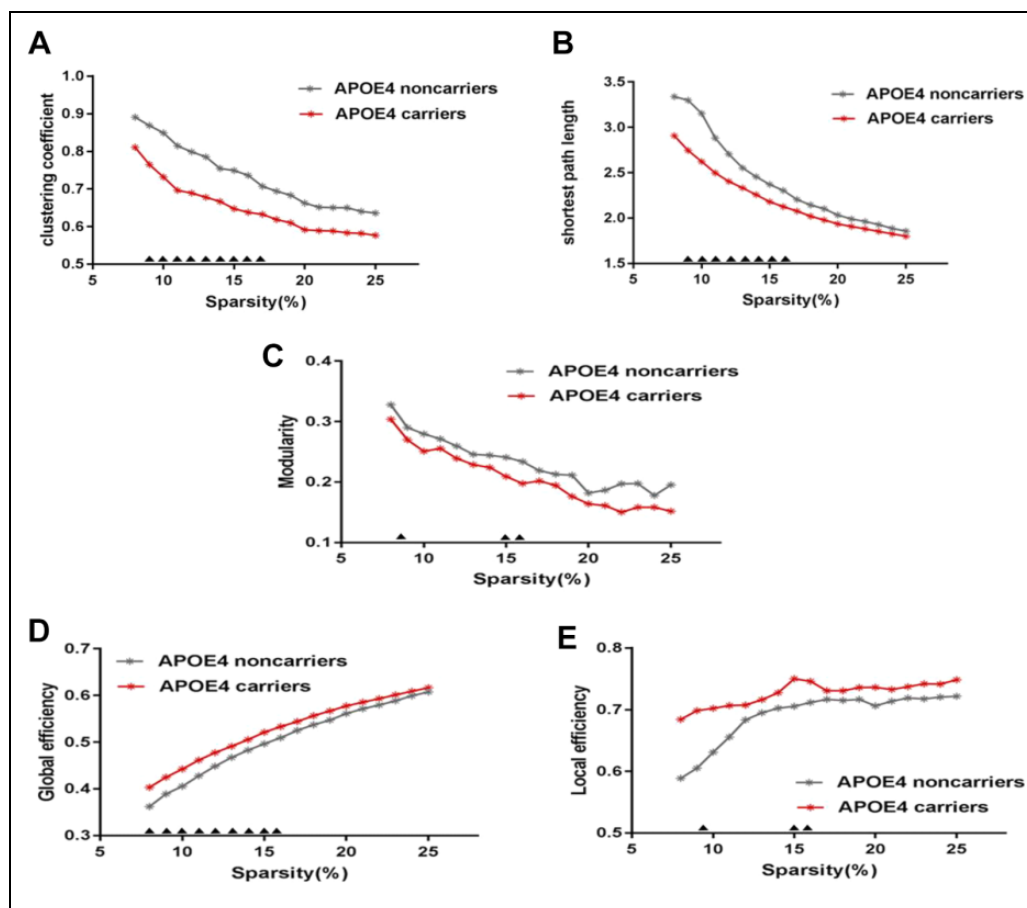
**Figure 2.** PHF-Tau network at different sparsity for APOE 4 carriers (the red line) and APOE 4 noncarriers (the gray line) and their statistical comparison results (p < 0.05 5000 permutation test, FDR correction). (A) clustering coefficient, (B) shortest path lenth, (C) Modularity, (D) global effciency, (E) local effciency. The black triangles indicate a significant group difference.
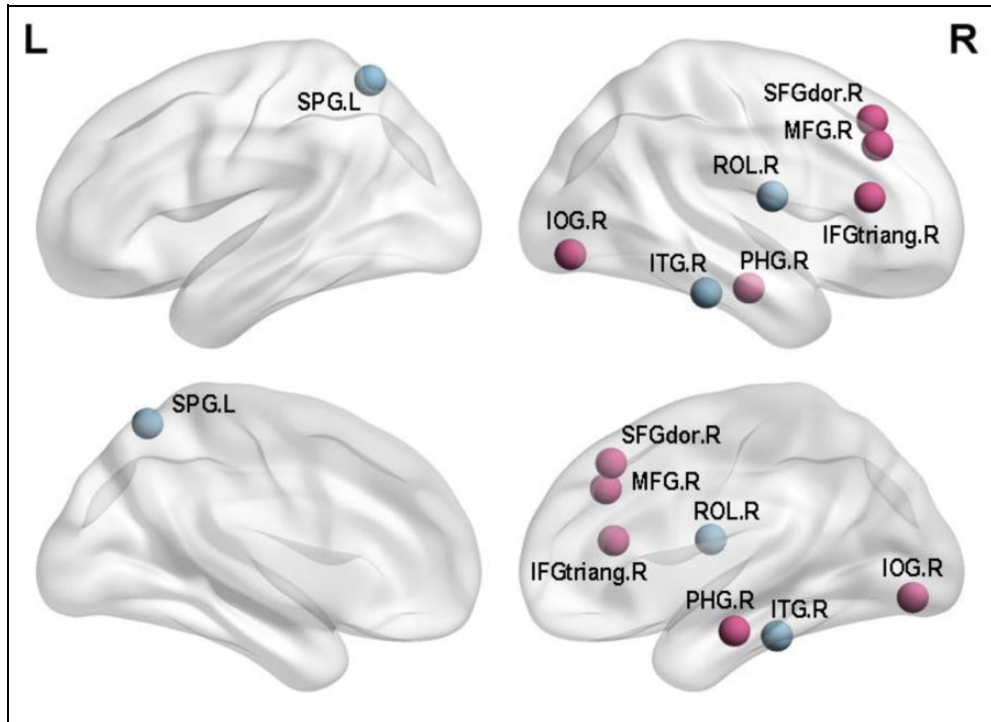
**Table 2.** Regions With Significant Differences in Nodal Efficiency Between APOE 4 Carriers and APOE 4 Noncarriers.

| Region | X | Y | Z | P-value |
|---|---|---|---|---|
| **Carriers >Noncarriers** | | | | |
| IFtriang.R | 140 | 141 | 93 | 0.0028 |
| SFGdor.R | 112 | 157 | 116 | 0.0066 |
| MFG.R | 128 | 159 | 106 | 0.0085 |
| IOG.R | 128 | 44 | 64 | 0.0099 |
| PHG.R | 115 | 111 | 52 | 0.0132 |
| **Carriers < Noncarriers** | | | | |
| ITG.R | 144 | 95 | 50 | 0.0169 |
| MTG.L | 34 | 92 | 70 | 0.0146 |
| SPG.L | 67 | 66 | 131 | 0.0247 |

## Tau Network Properties

Regarding global network topology, we found widespread changes in APOE 4 carriers. In previous researches, small-worldness losses were reported in the complex brain metabolic networks[24] and cortical networks.[25] Small-worldness property reflects the best balance between local specialization and global integration in brain networks.[26] The aforementioned abnormalities in small-worldness may indicate that the organization balance of PHF-tau network in APOE 4 carriers was disrupted, where PHF-tau network is turning to more randomly organized. There were also some alterations in the Cp, Lp, Eloc, Eglob, and Q value of modularity. The Cp reflected the degree of node aggregation, which was based on correlations between adjacent brain regions.[27] The APOE 4 carriers group exhibited the decreased Cp and a weaker local specialization, which suggested that Tau plaques aggregated together and transported to different brain regions easily.[28] Lp measured the ability of information transmission across brain regions. The decreased path length suggested a shorter information transmission path between 2 nodes.[29] Meanwhile, the alterations of Q value in modularity were found in the present study. This property reflects the ability of the network to process information within clusters of regions or modules.[30] The modularity assesses the extent to which a network can be divided into smaller communities of regions or modules that potentially share a specific function.[18] Moreover, the increased network efficiency may suggest the compensation mechanism of brain network to maintain the integrity of brain function.[31] Measures of network efficiency are related to cognitive control in MCI,

**Figure 3.** Regions with significant differences in nodal efficiency between APOE 4 carriers and APOE 4 noncarriers. Nonparametric permutation tests were applied to nodal efficiency of all 90 cortical regions (p < 0.05 5000 permutation test, FDR correction) (Purple for increased BC and blue for decreased BC).
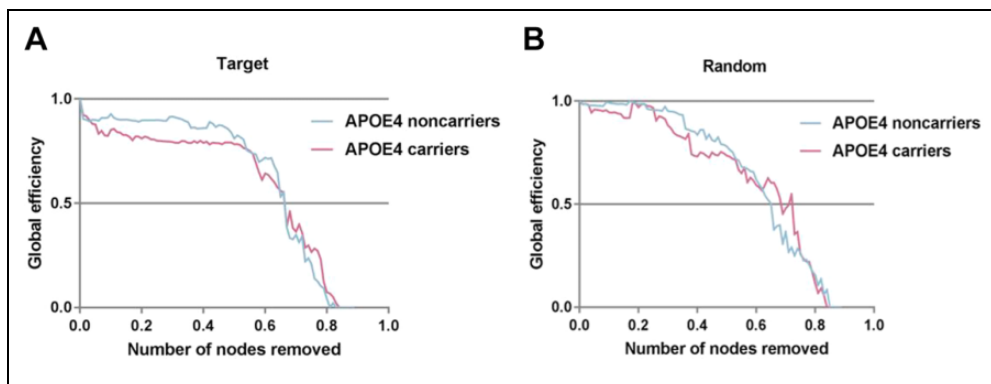


**Figure 4.** Network resilience under random and target analysis. The alterations of global efficiency under removing node at random (right panel) and targeted pattern (left panel). The purple line corresponded to the performance of APOE 4 carriers, blue line for APOE 4 noncarriers.

which is the reason that episodic memory deficits.[32] Aforementioned convergent evidences revealed that APOE 4 carriers are associated with disrupted global network organization and APOE 4 carriers with higher levels of cognitive impairment demonstrated greater alterations. These findings further underline that abnormal brain topology organization of PHF-Tau network is the main cause of cognitive control and situational memory deficit in MCI patients.

## Abnormal Changes in Nodal Centrality

The results showed that the significant increased regions in nodal centrality were located in right inferior frontal gyrus (triangular part), right superior frontal gyrus (dorsolateral), right middle frontal gyrus, right inferior occipital gyrus and right parahippocampal gyrus. Since the frontal lobe has been interpreted as being closely related to semantic processing and memory in the brain, the changed nodal centrality in the frontal lobe indicated that the abnormal Tau protein may influence memory impairment.[33] Fennemanotestine et al suggested that the APOE 4 allele might affect the cortical thickness of the frontal cortex, which is later developing regions and thought to be more effected on the natural aging process.[34] Espeseth et al indicated that a separate but partly overlapping right hemisphere system known as the ventral frontoparietal network included the temporoparietal junction would be effected by

APOE 4 allele, which was probably reflecting deficient attentional reorienting.[35] A finding proved that a reduction of resting glucose metabolism in frontal cortices was reported for APOE 4-carriers in brain regions known to be affected by MCI.[36] Several studies showed that abnormal frontal gray matter was associated with APOE 4 allele.[37,38] Moreover, A prior study have shown that compared with noncarriers, the volume of frontal and occipital lobes of APOE 4 carriers is abnormal.[39] Concomitant hypometabolism in occipital cortex was present in some of MCI/AD patients showing a more extended and severe cortical hypometabolism, which may aggravate cognitive impairment in these patients.[40] Increased Tau protein levels in occipital region had a significant pathological correlation with MCI and were also strongly correlated with the Braak stage.[41] Previous pathological aging study showed that parahippocampal volume as a biomarker has a better discriminatory effect than the volume of the hippocampus in differentiating MCI group from healthy control group.[42]

The significant decreased regions were found in nodal centrality were located in right inferior temporal gyrus, left middle temporal gyrus, left superior parietal gyrus. Metabolic dysfunction was most common in the temporal and parietal lobes associated areas, and metabolic decline in the medial parietal lobes seemed to more accurately distinguish between MCI patients and control participants.[43] The evidence showed that the inferior parietal cortices and medial temporal cortex are likely to be affected by tau accumulation.[44,45] Moreover, the middle temporal gyrus was associated with episodic memory abilities.[46] Previous studies suggested that these histopathological and volumetric changes in middle temporal gyrus are also associated with decreased performance on a wide range of memory tasks in older adults.[47,48] Neuroimaging showed medial temporal lobe atrophy in the early stage of the disease, while generalized temporal lobe and whole brain atrophy were the characteristics of MCI patients.[49] Such evidences, along with the results of this study indicated that the severity of clinical symptoms exhibited by MCI patients might be related to the levels of brain impairment. Therefore, abnormal Tau protein in the brain under the influence of APOE4 might accelerate the development of MCI.

### The Difference of Network Resilience

Through deleting the nodes and computing the global efficiency in the PHF-tau network, we assessed network resilience quantitatively (Figure 4). According to previous study,[20] the global efficiency would be more preferable as a measure of network integration than other network properties. As shown in Figure 4, PHF-tau networks in APOE 4 carriers were more vulnerable to perturbations or attacks. This finding enhanced the conclusion that the networks of APOE 4 carriers were less resilient than that of APOE 4 noncarriers.[50] Due to the power-law distribution, brain networks of the 2 groups are almost constant when deletion ratios is low.[51] As the deletion ratios reached 50%, the performance of both groups amalgamated. It is demonstrated that the topological structure of brain networks

is extremely disrupted and thus cannot support integrality.[14] From the perspective of the brain network, the effect of deleting nodes may indicate the cognitive decline of participants. This pattern have been found in other neurological diseases such as depression[50] and temporal lobe epilepsy.[22] Decreased attack survivability may reflect the topological reorganization of metabolic brain networks, providing insights into cognitive and memory impairments in APOE 4 carriers.

## Conclusion

In conclusion, this research tried to find the influences of APOE 4 on the Tau protein. Compared with the APOE 4 non-carriers, the APOE 4 carriers showed small- worldness losses and abnormal global topological organization in PHF-Tau network. The changed nodal centrality might indicate the neurobiological mechanisms underlying dementia cognitive dysfunction. In network resilience analysis, the brain network of APOE 4 carriers is more fragile. All in all, APOE 4 is an important factor that affects Tau neuron tangles and further impacts MCI or AD.

## Limitation

The present study had 2 limitations. Firstly, some of the moderating variables, such as average education years and intelligence quotient, were not collected in this analysis. Secondly, the study lacked participants with Alzheimer's disease, and no AD subjects made the analysis incomplete. Thirdly, in the future study, we will combine other factors which related to MCI into the research framework to explore the influence of different factors on Tau protein network. Finally, we will select more refined brain templates in constructing brain networks to reveal the deeper physiological mechanism.

## Funding

## ORCID iD

Bin Hu 🄳 https://orcid.org/0000-0003-3514-5413

## Supplemental Material

Supplemental material for this article is available online.

## References

1. Braak H, Braak E. Neuropathological stageing of Alzheimer-related changes. *Acta Neuropathol*. 1991;82(4):239-259.

2. Ward A, Tardiff S, Dye C, Arrighi HM. Rate of conversion from prodromal Alzheimer's disease to Alzheimer's dementia: a systematic review of the literature. *Dement Geriatr Cogn Dis Extra*. 2013;3(1):320-332.

3. Chien DT, Bahri S, Szardenings AK, et al. Early clinical PET imaging results with the novel PHF-tau radioligand [F-18]-T807. *J Alzheimer's Dis*. 2013;34(2):457-468.

4. Arnold SE, Lee EB, Moberg PJ, et al. Olfactory epithelium amyloid-β and paired helical filament-tau pathology in Alzheimer disease. *Ann Neurol*. 2010;67(4):462-469.

5. Yao Z, Hu B, Zheng J, et al. Initiative ASDN: a FDG-PET study of metabolic networks in apolipoprotein E ε4 allele carriers. *PLOS ONE*. 2015;10(7):e0132300.

6. Lehmann M, Ghosh PM, Madison C, et al. Greater medial temporal hypometabolism and lower cortical amyloid burden in ApoE4-positive AD patients. *J Neurol Neurosurg Psychiatry*. 2014;85(3):266-273.

7. Yao Z, Hu B, Hu T, An J, Song D, Zhong N. APOE4 modulates the activities within default mode network and interactions of resting intrinsic networks. In: *2017 IEEE International Conference on Bioinformatics and Biomedicine (BIBM)*: *2017*: IEEE; 2017:754-758.

8. Marquié M, Normandin MD, Vanderburg CR, et al. Validating novel tau positron emission tomography tracer [F-18]-AV-1451 (T807) on postmortem brain tissue. *Ann Neurol*. 2015;78(5): 787-800.

9. Cho H, Choi JY, Hwang MS, et al. Tau PET in Alzheimer disease and mild cognitive impairment. *Neurology*. 2016;87(4):375-383.

10. Olaf S, Chialvo DR, Marcus K, Hilgetag CC. Organization, development and function of complex brain networks. *Trends Cognitive Sci*. 2004;8(9):418-425.

11. Dicks E, Van der Flier WM, Barkhof F, Scheltens P, Tijms BM. Decline in grey matter connectivity over time is related to clinical progression in mci due to ad. *Alzheimer's Dementia*. 2018;14(7): P1479.

12. Wee CY, Yang S, Yap PT, Shen D. Sparse temporally dynamic resting-state functional connectivity networks for early MCI identification. *Brain Image Behavior*. 2016;10(2):342-356.

13. Khazaee A, Ebrahimzadeh A, Babajani-Feremi A. Classification of patients with MCI and AD from healthy controls using directed graph measures of resting-state fMRI. *Behavi Brain Res*. 2017; 322(Pt B):339-350.

14. Yao Z, Hu B, Chen X, et al. Learning metabolic brain networks in mci and ad by robustness and leave-one-out analysis: an FDG-PET Study. *Am J Alzheimer S Dis Other Dementias*. 2017;33(3): 153331751773153.

15. Sanabriadiaz G, Martínezmontes E, Meliegarcia L. Glucose metabolism during resting state reveals abnormal brain networks organization in the Alzheimer's disease and mild cognitive impairment. *Plos One*. 2013;8(7):e68860-e68860.

16. Watts DJ, Strogatz SH. Collective dynamics of 'small-world' networks. *Nature*. 1998;393(6684):440.

17. Latora V, Marchiori M. Efficient behavior of small-world networks. *Physical Rev Letters*. 2001;87(19):198701.

18. Newman ME, Girvan M. Finding and evaluating community structure in networks. *Physical Review. E Statist Nonlinear Soft Matter Physics*. 2004;69(2):026113.

19. Danon L, Diaz-Guilera A, Duch J, Arenas A. Comparing community structure identification. *J Statisti Mechani*. 2005; 2005(09):P09008.

20. Rubinov M, Sporns O. Complex network measures of brain connectivity: uses and interpretations. *Neuroimage*. 2010;52(3): 1059-1069.

21. Albert R, Jeong H, Barabasi AL. Error and attack tolerance of complex networks. *Nature*. 2000;340(1):378-382.

22. Bernhardt BC, Zhang C, Yong H, Evans AC, Neda B. Graph-theoretical analysis reveals disrupted small-world organization of cortical thickness correlation networks in temporal lobe epilepsy. *Cerebral Cortex*. 2011;21(9):2147-2157.

23. Yao Z, Zhang Y, Lei L, Yuan Z, Xu C, Jiang T. Abnormal cortical networks in mild cognitive impairment and Alzheimer's disease. *Plos Computati Biol*. 2010;6(11):e1001006-e1001006.

24. Bassett DS, Meyer-Lindenberg A, Achard S, Duke T, Bullmore E. Adaptive reconfiguration of fractal small-world human brain functional networks. *Proceedings Nati Acad Sci*. 2006;103(51): 19518-19523.

25. Yao Z, Zhang Y, Lin L, et al. Abnormal cortical networks in mild cognitive impairment and Alzheimer's disease. *PLoS Computati Biol*. 2010;6(11):e1001006.

26. Zhang J, Wang J, Wu Q, et al. Disrupted brain connectivity networks in drug-naive, first-episode major depressive disorder. *Biol Psychiatry* 2011;70(4):334-342.

27. Seo EH, Lee DY, Lee JM, et al. Whole-brain functional networks in cognitively normal, mild cognitive impairment, and Alzheimer's disease. *Plos One* 2013;8(1):e53922.

28. Duan H, Jiang J, Xu J, et al. Differences in AÎ² brain networks in Alzheimer's disease and healthy controls. *Brain Res*. 2017;1655: 77-89.

29. Sporns O, Zwi JD. The small world of the cerebral cortex. *Neuroinformatics*. 2004;2(2):145-162.

30. Haense C, Buerger K, Kalbe E, et al. CSF total and phosphory-lated tau protein, regional glucose metabolism and dementia severity in Alzheimer's disease. *Eur J Neurol Offic J Eur Federation Neurol Soc*. 2010;15(11):1155-1162.

31. Lou W, Shi L, Wang D, et al. Decreased activity with increased background network efficiency in amnestic MCI during a visuos-patial working memory task. *Human Brain Mapping*. 2015;36(9): 3387-3403.

32. Berlot R, Metzler-Baddeley C, Ikram MA, Jones DK, O'Sullivan MJ. Global efficiency of structural networks mediates cognitive control in mild cognitive impairment. *Frontiers Aging Neuroscie*. 2016;8:292.

33. Gabrieli JD, Desmond JE, Demb JB, et al. Functional magnetic resonance imaging of semantic memory processes in the frontal lobes. *Psychological Sci*. 1996;7(5):278-283.

34. Fennema-Notestine C, Panizzon MS, Thompson WR, et al. Presence of ApoE ε4 allele associated with thinner frontal cortex in middle age. *J Alzheimers Disease*. 2011;26(Suppl 3 26 Suppl 3):49-60.

35. Espeseth T, Westlye LT, Walhovd KB, et al. Apolipoprotein E ε4-related thickening of the cerebral cortex modulates selec-tive attention. *Neurobiology of Aging*. 2012;33(2):304-322. e301.

36. Filippini N, MacIntosh BJ, Hough MG, et al. Distinct patterns of brain activity in young carriers of the APOE-ε4 allele. *Proceed-ings National Academy Sci*. 2009;106(17):7209-7214.

37. Yasuda M, Mori E, Kitagaki H, et al. Apolipoprotein E epsilon 4 allele and whole brain atrophy in late-onset Alzheimer's disease. *Am J Psychiatry*. 1998;155(6):779.

38. Geroldi C, Laakso MP, Decarli C, et al. Apolipoprotein E genotype and hippocampal asymmetry in Alzheimer's disease: a volumetric MRI study. *J Neurol Neurosurgery Psychiatry*. 2000;68(1):93-96.

39. Borghesani PR, Johnson LC, Shelton AL, et al. Altered medial temporal lobe responses during visuospatial encoding in healthy APOE*4 carriers. *Neurobiol Aging*. 2008;29(7):981-991.

40. Morbelli S, Bauckneht M, Arnaldi D, et al. 18F–FDG PET diag-nostic and prognostic patterns do not overlap in Alzheimer's dis-ease (AD) patients at the mild cognitive impairment (MCI) stage. *Eur J Nuclear Med Molecular Imaging*. 2017;44(12):2073-2083.

41. Schwarz AJ, Yu P, Miller BB, et al. Regional profiles of the candidate tau PET ligand 18 F-AV-1451 recapitulate key features of Braak histopathological stages. *Brain*. 2016;139(5):1539-1550.

42. De T-ML, Goncharova I, Dickerson B, Wilson RS, Bennett DA. From healthy aging to early Alzheimer's disease: in vivo detec-tion of entorhinal cortex atrophy. *Ann N Y Acad Sci*. 2010;911(1): 240-253.

43. Villain N, Fouquet M, Baron J-C, et al. Sequential relationships between grey matter and white matter atrophy and brain meta-bolic abnormalities in early Alzheimer's disease. *Brain*. 2010; 133(11):3301-3314.

44. Cho H, Choi JY, Hwang MS, et al. In vivo cortical spreading pattern of tau and amyloid in the Alzheimer disease spectrum. *Ann Neurol*. 2016;80(2):247-258.

45. Johnson KA, Schultz A, Betensky RA, et al. Tau positron emis-sion tomographic imaging in aging and early Alzheimer disease. *Ann Neurol*. 2016;79(1):110-119.

46. Bub D. Review of Handbook of functional neuroimaging of cog-nition. *Canadian Psychol*. 2002;42(4):318-320.

47. Mori E, Yoneda Y, Yamashita H, Hirono N, Ikeda M, Yamadori A. Medial temporal structures relate to memory impairment in Alzheimer's disease: an MRI volumetric study. *J Neurol Neurosurgery Psychiatry*. 1997;63(2):214-221.

48. Mirrashed F. Verbal episodic memory impairment in Alzheimer's disease: a combined structural and functional MRI study. *Neuroimage*. 2005;25(1):253-266.

49. Fox N, Warrington E, Freeborough P, et al. Presymptomatic hip-pocampal atrophy in Alzheimer's disease: a longitudinal MRI study. *Brain*. 1996;119(6):2001-2007.

50. Ajilore O, Lamar M, Leow A, Zhang A, Yang S, Kumar A. Graph theory analysis of cortical-subcortical networks in late-life depression. *Am J Geriatric Psychiatry*. 2014;22(2):195-206.

51. Friedman EJ, Landsberg AS. Hierarchical networks, power laws, and neuronal avalanches. *Chaos*. 2013;23(1):187-203.